

Ferroelectricity and tetragonality in ultrathin PbTiO₃ films

Céline Lichtensteiger* and Jean-Marc Triscone

DPMC - Université de Genève, 24 Quai Ernest-Ansermet, CH-1211 Genève 4, Switzerland

Javier Junquera† and Philippe Ghosez

Département de Physique, Université de Liège, B-4000 Sart-Tilman, Belgium

(Dated: March 14, 2019)

The evolution of tetragonality with thickness has been probed in epitaxial c-axis oriented PbTiO₃ films with thicknesses ranging from 500 down to 24 Å. High resolution x-ray pointed out a systematic decrease of the c-axis lattice parameter with decreasing film thickness below 200 Å. Using a first-principles model Hamiltonian approach, the decrease in tetragonality is related to a reduction of the polarization attributed to the presence of a residual unscreened depolarizing field. It is shown that films below 50 Å display a significantly reduced polarization but still remain ferroelectric.

PACS numbers: 77.80.-e, 31.15.Ar, 77.84.Dy, 77.84.-s, 81.15.-z

Since its discovery in 1920 by Valasek [1], ferroelectricity has attracted considerable interest from a fundamental point of view and because of its wide range of potential applications. Ferroelectricity has been historically seen as a *collective* phenomenon [2] requiring a relatively large critical volume of aligned dipoles, rather than an assembly of independent polar entities. Calculations within the Ginzburg-Landau theory had indicated that, as the physical dimensions of a ferroelectric material are reduced, the stability of the ferroelectric state is altered, leading to a relatively large critical size below which ferroelectricity is suppressed in small particles and thin films [3, 4]. For instance, in the case of Pb(Zr_{0.5}Ti_{0.5})O₃ thin films, a critical thickness of ~200 Å had been predicted at room temperature [4]. These predictions appeared to agree with then-current experiments [5]. Recent results, however, suggest a much smaller critical size, with ferroelectricity detected in polymer films down to 10 Å [6] and in perovskite films down to 40 Å (10 unit cells) [7]. Very recently, x-ray synchrotron studies have revealed periodic 180° stripe domains in 16 to 420 Å thick epitaxial films of PbTiO₃ (PTO) grown on insulating SrTiO₃ (STO) substrates [8]. On the theoretical side, atomistic simulations have emphasized the predominant role of *electrostatic* boundary conditions to control ferroelectricity in very thin films. Ghosez and Rabe [9], and Meyer and Vanderbilt [10] showed that, under perfect screening of the depolarizing field, ultrathin stress-free perovskite free-standing slabs can sustain a polarization perpendicular to the surface. However, perfect screening is not achieved in usual ferroelectric capacitors, and the residual depolarizing field can substantially affect the ferroelectric properties [11]. Recently, the consequences of imperfect screening on the coercive field have been studied in detail [12]. Also, first principles calculations al-

lowed the amplitude of the depolarizing field for BaTiO₃ ultrathin films between metallic SrRuO₃ electrodes in short-circuit conditions to be quantified and a critical thickness of ~24 Å (6 unit cells) in such structures to be predicted [13].

These recent experimental and theoretical results, at odds with the former well established belief, clearly show that additional studies are crucial to demonstrate experimentally the key role of screening and confirm ferroelectricity at the nanoscale [14]. In this Letter we report on combined experimental and theoretical investigations of tetragonality in a series of epitaxial c-axis oriented films of PTO grown onto metallic Nb-doped STO substrates. X-ray analyses show that the tetragonality progressively *decreases* below 200 Å. Using a first-principles-based model Hamiltonian approach, we relate this lowering of *tetragonality* to a lowering of the spontaneous *polarization* of the films, due to a residual unscreened depolarizing field as predicted in Ref. 13. Our results show that ultrathin PTO films on Nb-STO display a significantly reduced spontaneous polarization but still remain ferroelectric below 50 Å.

The PTO films were grown onto metallic (001) Nb-STO substrates by off-axis radio-frequency (RF) magnetron sputtering [15]. During sputtering, a flux composed of 33 sccm of argon and 14 sccm of oxygen was introduced in the chamber while the process pressure was maintained at 180 mTorr. The substrate was heated up to 475–485°C, as measured by a pyrometer. Two series of films were grown using RF powers of 60W and 40W applied to the Pb_{1.1}TiO₃ target, corresponding to growth rates of 280 Å/h and 110 Å/h respectively [26].

Room temperature x-ray measurements, using a *Philips X'Pert High Resolution* diffractometer, allowed us to determine precisely the epitaxy of the films, their thickness and their c-axis parameter. The θ - 2θ diffractograms, revealing only (00l) reflections, demonstrate that the films are purely c-axis with the polarization normal to the film surface. Pole-figures confirmed the expected epitaxial “cube on cube” growth and that the films were tetragonal. Typical high resolution θ - 2θ low

*Electronic address: Celine.Lichtensteiger@physics.unige.ch

†Present address : Department of Physics and Astronomy, Rutgers University, Piscataway, NJ 08854-8019, USA

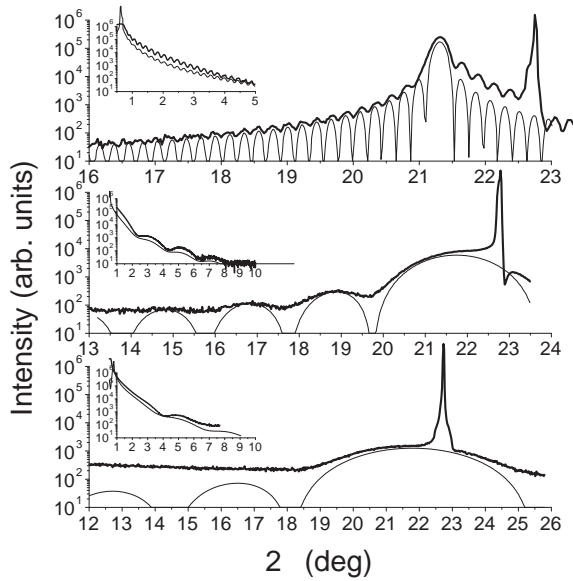


FIG. 1: Room temperature low and high angle x-ray diffraction measurements (thick lines) and simulations (thin lines) for three samples of 390 Å (top), 44 Å (middle) and 24 Å (bottom). The c-axis values used for these simulations are $c=4.17$ Å (top), $c=4.09$ Å (middle) and $c=4.07$ Å (bottom).

and high angle scans are shown on Fig. 1 revealing the thin high intensity substrate diffraction peaks as well as the broader film diffraction peaks. High angle finite size oscillations and low angle reflectometry (see insets of Fig. 1) allowed us to determine, through simulations, the number of planes involved in the diffraction and thus the film thickness [16] as well as the deposition rate, even for films down to 24 Å. Since the a-axis lattice parameter of ferroelectric bulk PTO is 3.902-3.904 Å [17, 18], very close to the 3.905 Å of the STO, the films are expected to be coherent with their a-axis equal to the STO lattice parameter. Grazing incidence diffraction on a ~ 86 Å thin film confirmed this picture displaying a unique (200) reflection. Measurements of the PTO (101) reflection for the thickest films (~ 504 Å and ~ 396 Å) gave an estimation of $a = 3.90 \pm 0.01$ Å. For these films, in-plane strain relaxation would lead to a maximum change in the c-axis length of 0.006 Å, which is ~ 15 times smaller than the changes observed and discussed below.

To probe finite size effects in thin films, a key requirement is to have materials with smooth surfaces, and therefore a well-defined thickness. In order to get information about the surface quality of the films, atomic force microscope (AFM) topographic measurements were performed on all the samples, showing that the films are essentially atomically smooth with a root-mean-square (RMS) roughness between 2 and 6 Å over $10 \times 10 \mu\text{m}^2$ areas. Fig. 2(A) shows representative topographic im-

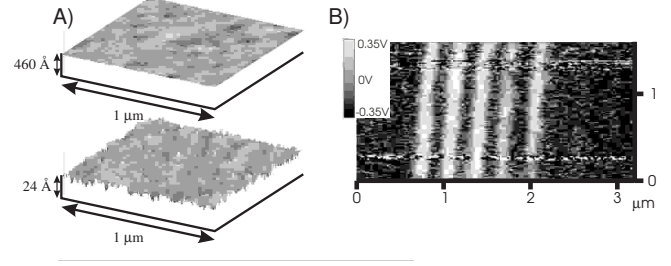


FIG. 2: A) AFM topographies for 460 Å (top) and 24 Å (bottom) thick films. The vertical scale is the film thickness and the RMS values measured over $10 \times 10 \mu\text{m}^2$ areas are 2 Å and 3 Å respectively. B) Piezoresponse signal obtained after writing ten stripes using alternate +12V and -12V voltages applied to the tip.

ages obtained for scan areas of $1 \mu\text{m}^2$ on two PTO thin films. The vertical scale used in these 3D representations is equal to the respective thickness of each sample, allowing a comparison of the roughness of the surface with the total film thickness. As can be seen from the data, the average thickness remains well defined, even for ultrathin films down to 6 unit cells.

Finally, we used the piezoresponse mode of the AFM to probe the domain structure of different films [19, 20]. Ten stripes were drawn using alternate +12V and -12V voltages applied to the tip over a $1.6 \times 1.6 \mu\text{m}^2$ area. In Fig. 2(B), the $3.2 \times 1.6 \mu\text{m}^2$ background piezoresponse signal containing the written stripes was then compared to the signal from the stripes, and found to be equal to the signal obtained for the +12V written stripes suggesting a single polarization in the as grown sample. All the investigated films were found to be “monodomain-like” over the studied areas, typically a few μm^2 .

We now return to the relation between the c-axis parameter and the film thickness. Fig. 3 shows the central result of the paper : the film tetragonality, i.e. the c/a ratio, is plotted as a function of film thickness for the two series of samples (top). To precisely determine the c-axis parameter, we performed x-ray diffraction for the $(00l)$, $l=1$ to 5 reflections. The a-axis value is taken as constant and equal to 3.905 Å. As can be seen, the data for both series collapse and the c/a ratio decreases very substantially for films thinner than 200 Å.

We also note that a very similar reduction of tetragonality has recently been observed by Tybella [21]. It has also been checked experimentally that the c-axis values did not change after the deposition of a gold electrode and shortening of the gold electrode and the metallic substrate (insuring short circuit conditions).

The observed reduction of c/a shown on Fig. 3 (top) cannot be attributed to a change in the a-axis lattice parameter since it is independent of the film thickness. Instead, the decrease of c must be related to a concomitant reduction of the spontaneous polarization through the

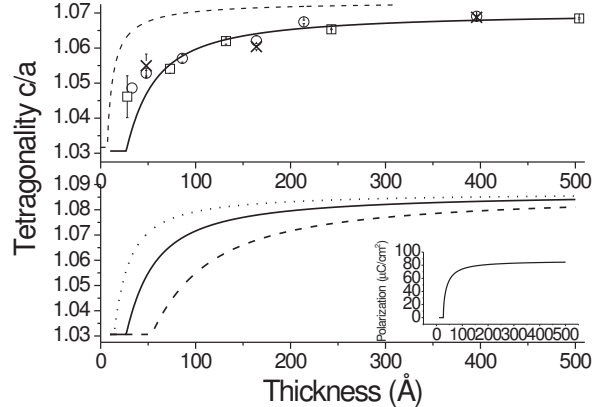


FIG. 3: Evolution of the c/a ratio with the film thickness. Top: experimental results for the 1st series (circles), the 2nd series (squares), and the 1st series with a gold top electrode (crosses); the dashed line is the phenomenological theory prediction (see main text) supposing a ratio between the extrapolation and the correlation length $\delta/\xi = 1.41$ [22]; the solid line is the model Hamiltonian prediction for $\lambda_{eff}=0.12$ Å, rescaled to give a maximum tetragonality in agreement with the experimental data. Bottom: results from the model Hamiltonian calculations for $\lambda_{eff}=0.23$ Å (dashed line), $\lambda_{eff}=0.12$ Å (solid line) and $\lambda_{eff}=0.06$ Å (dotted line). Inset: thickness dependence of the spontaneous polarization from the model Hamiltonian for $\lambda_{eff}=0.12$ Å.

polarization-strain coupling that is known to be particularly large in PTO [23]. The evolution of c/a therefore is a signature of the progressive suppression of ferroelectricity in ultrathin films as predicted in Ref. 13.

This can be highlighted theoretically by extending the first-principles effective Hamiltonian approach developed by Waghmare and Rabe for bulk PTO [24] to thin films. Within this approach, the energy is written as a low-order Taylor expansion of the bulk energy around the cubic phase within the restricted subspace spanned by (i) the ionic degree of freedom ξ associated to the lattice Wannier function of the soft phonon branch and (ii) the macroscopic strain e . The Hamiltonian includes three terms : the double-well soft-mode energy, the elastic energy and a coupling term between ξ and e .

In Ref. 13, the suppression of the ferroelectricity in ultrathin films between metallic electrodes in short-circuit was related to the *incomplete* screening of the depolarizing field by the electrodes. It was also shown that the energetics of ultrathin films can be reasonably described using a simple model that corrects the bulk internal energy at first order by a term taking into account the energy associated to the coupling between the polarization \mathcal{P} and the unscreened depolarizing field \mathcal{E}_d . Transposing this to the effective Hamiltonian approach allows us to

write :

$$\mathcal{H}_{eff}^{film}[\xi, e] = \mathcal{H}_{eff}^{bulk}[\xi, e] - \mathcal{E}_d \cdot \mathcal{P} \quad (1)$$

where \mathcal{H}_{eff}^{bulk} and \mathcal{H}_{eff}^{film} are the model Hamiltonians for bulk and thin films respectively. For \mathcal{H}_{eff}^{bulk} , we keep the form and parameters fitted at the experimental volume as reported in Ref. 24. Therefore, the only finite-size correction included in \mathcal{H}_{eff}^{film} arises from the electrostatic energy related to \mathcal{E}_d .

It follows from Ref. 13 that, under short circuit conditions, \mathcal{E}_d is related to the potential drop ΔV at each metal/ferroelectric interface. Assuming two similar interfaces with the top and bottom electrodes, then $\mathcal{E}_d = -2\Delta V/d$, where d is the thickness of the film. The potential drop was attributed to finite dipoles at the interfaces and was shown to evolve *linearly* with the spontaneous polarization : $\Delta V = (\lambda_{eff}/\epsilon_0) \cdot \mathcal{P}$. The parameter λ_{eff} has the dimension of a length and will be referred to as the *effective* screening length of the system [25].

Supposing monodomain films polarized along z , in agreement with the piezoresponse measurements, the macroscopic polarization is homogeneous and directly linked to ξ ($\mathcal{P}_z = Z^* \xi_z / \Omega_0$ [24] where Z^* is the soft mode effective charge, ξ_z is the z -component of ξ , and Ω_0 is the unit cell volume) so that we finally obtain :

$$-\mathcal{E}_d \cdot \mathcal{P}_z = (2\lambda_{eff} Z^{*2} / \Omega_0^2 \epsilon_0 d) \xi_z^2 \quad (2)$$

This energy scales with λ_{eff}/d and is *positive* meaning that the effect of the depolarizing field is to suppress the ferroelectric instability through a renormalization of the quadratic term of the effective Hamiltonian.

The previous model is now applied to thin films of PTO on Nb-STO. Perfect pseudomorphic thin films on top of a cubic substrate are considered and the in-plane strains ($e_{xx} = e_{yy}$) are fixed throughout the structure independently of the film thickness, in order to constrain the a -axis lattice constant imposed by the STO substrate (3.905 Å) [27]. The energy (Eq. 1) is then minimized for different thicknesses in terms of ξ_z (supposed uniform and perpendicular to the film) and e_{zz} . From the values of ξ_z and e_{zz} we deduce \mathcal{P} and c/a . All the simulations have been carried out at $T = 0$.

The fit of first-principles results for the $\text{SrRuO}_3/\text{BaTiO}_3$ interface [13] yields $\lambda_{eff} = 0.23$ Å. Because the screening might be slightly different for the present system composed of distinct interfaces, the theoretical results are reported in Fig. 3 (bottom) for slightly different values of λ_{eff} . The model predicts a critical thickness below which the spontaneous polarization vanishes and the c/a ratio of the resulting paraelectric phase saturates at 1.03, as a result of the mechanical constraint imposed by the substrate. Above the critical thickness, the spontaneous polarization gradually increases up to the bulk value as does the c -axis lattice parameter, consequently to the polarization-strain coupling.

The model Hamiltonian of Waghmare and Rabe, although appropriately describing PTO, is known to overestimate the polarization-strain coupling. At the bulk level, the model predicts $c/a = 1.09$ while the experimental value is equal to ~ 1.06 [24]. In order to get rid of this bulk overestimation, and for a direct comparison of the theoretical and experimental *evolution* of c/a , the theoretical curves have been renormalized to give a tetragonality of 1.068 at 500 Å, in agreement with the experimental data. Only the strength of the polarization-strain coupling must be rescaled while the c/a value of the paraelectric phase, a priori properly predicted through the elastic constants, can be kept unchanged.

Looking at the experimental points on Fig. 3 (top), both the *range* of thicknesses at which the c/a ratio starts to decrease and the *shape* of the evolution agree with the prediction of the model Hamiltonian calculations for $\lambda_{eff} = 0.12$ Å. This supports an incomplete screening of the depolarizing field as the driving force for a global reduction of the polarization in perovskite ultrathin films. In contrast, the Devonshire-Ginzburg-Landau phenomenological theory which includes only an intrinsic suppression of ferroelectricity at the surface through the so-called extrapolation length parameter δ [22] predicts a much sharper decay with no substantial decrease of polarization predicted above 50 Å, not borne out by the experimental observations.

The value of λ_{eff} (0.12 Å) used in Fig. 3 (top) is smaller than in the case of the BaTiO₃/SrRuO₃ interface [13] (0.23 Å). This might suggest a better screening for the present system but might also be partly attributed to an overestimate of the theoretical critical thickness due to the simplicity of the model Hamiltonian [28] and to the

fact that the simulations were performed at T=0.

Importantly, the thinnest films have a much higher tetragonality than the value of 1.03 expected for the paraelectric phase from the macroscopic theory of elasticity. No saturation of c/a , the signature of a complete suppression of ferroelectricity, was experimentally identified, clearly implying that films much thinner than 50 Å are still ferroelectric.

In conclusion, we found that the c-axis parameter of PTO films decreases substantially below 200 Å. A first-principles effective Hamiltonian approach allowed us to establish that the lowering of c/a is related to a progressive reduction of the polarization due to an imperfect screening of the depolarizing field. The fact that no saturation of the c-axis value was found down to very thin films (24 Å) demonstrates that films below 50 Å remain ferroelectric at room temperature, although with a significantly reduced polarization.

Acknowledgements : We would like to thank A. García and K. M. Rabe for helpful discussions, S. Gariglio and E. Koller for their x-ray diffraction expertise, P. Paruch for a careful reading of the manuscript, and D. Chablaix and the whole Geneva workshop for very efficient technical support. This work was supported by the Swiss National Science Foundation through the National Center of Competence in Research “Materials with Novel Electronic Properties-MaNEP” and Division II, the VolkswagenStiftung within the project “Nanosized ferroelectric hybrids” (I/77 737), NEDO, FNRS-Belgium (grants 9.4539.00 and 2.4562.03) and ESF (Thiox). JJ acknowledges financial support from the Fundación Ramón Areces and the Spanish MCyT Grant No. BFM2000-1312.

[1] J. Valasek, Phys. Rev. **15**, 537 (1920).
[2] M. E. Lines and A. M. Glass, *Principles and applications of ferroelectrics and related materials* (Oxford University Press, Oxford, 1977).
[3] S. Li *et al.*, Phys. Lett. A **212**, 341 (1996).
[4] S. Li *et al.*, Jpn. J. Appl. Phys. **36**, 5169 (1997).
[5] J. F. Scott *et al.*, Physica B **150**, 160 (1988).
[6] A. Bune *et al.*, Nature (London) **391**, 874 (1998).
[7] T. Tybell, C. H. Ahn, and J.-M. Triscone, Appl. Phys. Lett. **75**, 856 (1999).
[8] S. Streiffer *et al.*, Phys. Rev. Lett. **89**, 067601 (2002).
[9] P. Ghosez and K. M. Rabe, Appl. Phys. Lett. **76**, 2767 (2000).
[10] B. Meyer and D. Vanderbilt, Phys. Rev. B **63**, 205426 (2001).
[11] R. R. Mehta, B. D. Silverman, and J. T. Jacobs, J. Appl. Phys. **44**, 3379 (1973).
[12] M. Dawber *et al.*, J. Phys.: Condens. Matter **15**, L393 (2003).
[13] J. Junquera and P. Ghosez, Nature (London) **422**, 506 (2003).
[14] For a recent review on nanoscale ferroelectrics, see C. H. Ahn, K. M. Rabe, and J.-M. Triscone, Science **303**, 488 (2004).
[15] C.-B. Eom, Ph.D. thesis, Stanford University (1991).
[16] See, for instance, J.-M. Triscone *et al.*, Phys. Rev. B **50**, 1229 (1994).
[17] R. Nelmes and W. Kuhs, Solid State Commun. **54**, 721 (1985).
[18] J. Joseph *et al.*, J. Mater. Science **35**, 1571 (2000).
[19] T. Tybell, C. H. Ahn, and J.-M. Triscone, Appl. Phys. Lett. **72**, 1454 (1998).
[20] A. K. S. Kumar *et al.*, to be published in Ferroelectrics .
[21] T. Tybell, (2003), private communication.
[22] A. Zembilgotov *et al.*, J. Appl. Phys. **91**, 2247 (2002).
[23] R. E. Cohen, Nature (London) **358**, 136 (1992).
[24] U. Waghmare and K. M. Rabe, Phys. Rev. B **55**, 6161 (1997).
[25] J. Junquera, K. M. Rabe, and P. Ghosez (2003), unpublished.
[26] Higher growth rates were observed for ultrathin films (below 40 Å).
[27] Within \mathcal{H}_{eff} , the strains are defined with reference to the bulk cubic structure of PTO so that the epitaxial growth imposes $e_{xx} = e_{yy} = (a_{STO} - a_{PTO})/a_{PTO}$ with $a_{STO} = 3.905$ Å and $a_{PTO} = 3.969$ Å.

[28] A similar model for BaTiO₃ predicts a critical thickness of 35 Å, larger than the first-principles value of 24 Å reported in Ref. 13.